MATERIALS PERSPECTIVE

Aberration corrected and monochromated environmental transmission electron microscopy: challenges and prospects for materials science

T. W. Hansen*, J. B. Wagner and R. E. Dunin-Borkowski

The latest generation of environmental transmission electron microscopes incorporates aberration correctors and monochromators, allowing studies of chemical reactions and growth processes with improved spatial resolution and spectral sensitivity. Here, we describe the performance of such an instrument using examples taken from studies of fuel cells and supported catalysts. We discuss the challenges involved in performing *in situ* gas reaction experiments quantitatively and reliably and we highlight the care required to understand the effect of the electron beam on dynamic experiments performed in the electron microscope.

Keywords: Environmental transmission electron microscopy, Aberration correction, Monochromation, Catalysis, Fuel cells, Electron energy-loss spectroscopy, Nanoparticles

Introduction

Traditionally, transmission electron microscopy (TEM) has been a high vacuum discipline. However, in both academic and industrial research, there is now an increasing need to expose samples to more realistic environments during image acquisition, in the form of gas mixtures and elevated temperatures. This technique has been known as controlled atmosphere TEM[1] and, more recently, as *in situ* TEM or environmental TEM (ETEM).[2] The demand for instruments with *in situ* or environmental capabilities is strong. The catalysis[3] and semiconductor[4] communities, in particular, have highlighted the need for investigating materials under the conditions in which they operate in order to overcome the drawbacks of post-mortem studies, in which samples are transferred to microscope facilities after *ex situ* reactions.

In the 1950s and the following decades, Hashimoto and Naiki[5] designed and developed the first gas reaction specimen chamber based on the differential pumping concepts that are used in today's ETEMs. A chamber of this design was used by Baker and co-workers in the 1970s, primarily to investigate particle mobility and carbon filament growth in supported metal catalysts.[1,6,7] The primary difference between this early environmental cell and the design that is used today is that in the present design, the cell is integrated into the column, providing better stability and flexibility. An account of recent results and performance from state-of-the-art ETEMs can be found in a review by Sharma.[8]

Center for Electron Nanoscopy, Technical University of Denmark, DK-2800 Kongens Lyngby, Denmark

*Corresponding author, email twh@cen.dtu.dk

Recently, the availability of aberration correction and monochromation on commercial TEMs has significantly improved interpretable spatial resolution to the sub-angstrom level[9] and reduced image delocalisation. These developments allow images of surface and interface structures, which are of paramount importance for catalysis, to be acquired and interpreted more easily.[10] The energy resolution in electron energy-loss spectroscopy (EELS) has also been improved by the introduction of monochromators, a concept that dates back to the 1960s,[11] but which can be used to bring energy spread down to below a few hundred meV.[12,13] The combination of *in situ* TEM and monochromation now allows high resolution EELS to be performed during gas and/or temperature induced phase transitions.

Microscope configuration

The present review is based on the ETEM installed at the Center for Electron Nanoscopy in the Technical University of Denmark (DTU Cen), but the requirements and concerns described here are generally applicable to all types of ETEMs.

The Titan platform from FEI forms the basis of the ETEM at DTU Cen. A three-condenser lens system and a stabilised column on a standard FEI Titan 80-300 are supplemented by a monochromator and a corrector of the spherical aberration coefficient C_S of the microscope objective lens. When the microscope is operated at an acceleration voltage of 300 kV, the monochromator provides a measured energy spread of better than 200 meV (in high vacuum operating mode), measured as the full width at half maximum of the zero loss peak for the shortest possible acquisition time. Without aberration correction, the point resolution and information limit are

Published by Maney on behalf of the Institute
Received 4 May 2010; accepted 14 June 2010
DOI 10.1179/026708310X12756557336355

0·2 and <0·1 nm respectively.[14] The C_S image corrector brings the point resolution down to below 0·1 nm when the microscope is operated at 300 kV.

Integration of environmental capabilities

In order to minimise the scattering of electrons by gas molecules in the high pressure (7 mm) region of the microscope, the distance that the electron beam travels through the gas should be as short as possible. At the same time, the pole piece gap has to be large enough to allow flexibility of specimen holder design and to provide space for high specimen tilt angles for electron tomography.

The introduction of gases into the electron microscope column increases the need for pumping capacity. The ETEM at DTU Cen is based on a design developed by Boyes and Gai[2] in collaboration with Philips. The TEM column is differentially pumped in several stages using both turbomolecular and ion getter pumps, which allow high vacuum to be maintained at the electron source. Figure 1 shows the design of the microscope column. Each pumping stage is separated by additional apertures that result in pressure drops. For a pressure of ~1500 Pa in the sample region, the pressure is ~1 Pa after the first pumping stage and $\sim 10^{-3}$ Pa after the second stage. The pressure in the field emission gun region remains below 10^{-6} Pa.

The pumping pathways for the first differential pumping stage are created by drilling holes through the pole pieces of the TEM objective lens. In order to retain the performance of the lens, the modification is made in a symmetrical manner, with dummy holes drilled opposite to the pumping pathways. This design allows a pressure of up to ~2000 Pa (depending on gas composition) to be maintained around the sample (between the pole pieces, limited by the first set of differential pumping apertures).

The microscope can be operated in two primary modes. During conventional operation, the column is pumped using the standard ion getter pumps. In this mode, the exhausts to the turbomolecular pumps are sealed from the column by ultrahigh vacuum compatible pneumatic gate valves, and the microscope operates as a conventional C_S image corrected monochromated Titan with a slightly lower maximum cutoff angle for detecting high angle scattering. When carrying out environmental experiments (in ETEM mode), the pumping pathways to the ion getter pumps in the specimen area are sealed off, and the valves to the three turbomolecular pumps are opened to provide the pumping capacity needed. Furthermore, a port providing direct access to the sample region can be opened, allowing gas injection around the specimen. The differential pumping scheme on the FEI Titan column is designed with an emphasis on exposing samples to as high a pressure as possible while maintaining a large pole piece gap and the high resolution capabilities of the microscope during imaging.

The pressure in the sample region depends on diffusion through the pumping apertures. Even before introducing gas into the column, the base pressure in the sample region in ETEM mode is therefore higher than in conventional high vacuum mode (when the ion getter pumps are applied directly to the specimen area). This design makes the present microscope less suitable for low pressure ETEM studies than a dedicated ultrahigh vacuum microscope with an *in situ* capability.[15–18]

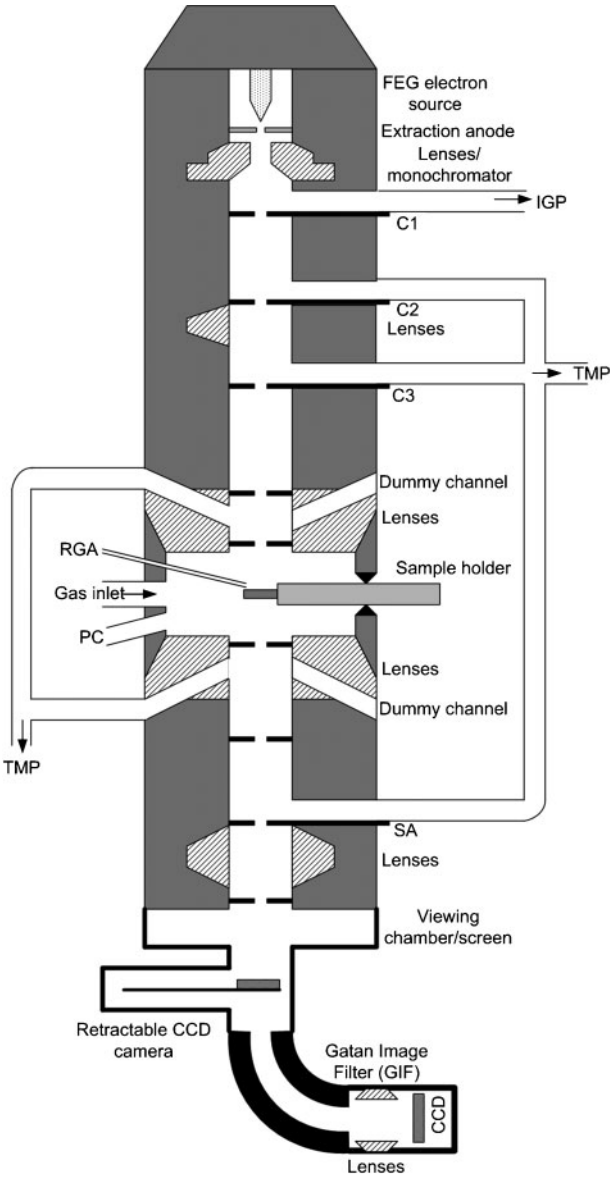

1 Schematic diagram of differentially pumped TEM column (FEG, field emission gun; IGP, ion getter pump; TMP, turbomolecular pump; RGA, residual gas analyser; PC, plasma cleaner; C1, first condenser aperture; SA, selected area aperture)

Gas inlet system

Specimen drift has to be minimised when gas–solid reactions are followed in an electron microscope. During typical experiments, gas–solid interactions are followed over extended periods of time with the specimen held at elevated temperature, for example by using a heating specimen holder that has a current running through a filament. When the holder and the specimen are surrounded by gas, both heat transfer to the gas and the temperature to which the specimen can be heated depend strongly on gas pressure and composition. In the past, heating holders consisted of a furnace with a resistively heated filament onto which the sample was clamped. As the heating power in these compact filaments is small, the temperature that can be reached is highly dependent on the gas pressure and composition

in the sample region. As small variations in gas pressure can then result in large variations in specimen temperature, the gas flow in the sample region must be highly stable. This requirement is realised by maintaining a constant gas flow through the system. The first differential pumping apertures act as the limiting factor for gas flow out of the sample region. The pressure that builds up in the sample region then depends primarily on the flow into the column when the gas composition is kept fixed. Thus, to keep a stable pressure and subsequently a stable temperature around the sample, a high degree of control over the gas flow is essential. Failure to provide a stable gas feed can result in specimen drift and loss of image resolution.

Recently, heating holders that utilise microelectromechanical systems (MEMS) technologies have become available. In such holders, the heating filament is in close proximity to the specimen, and heating rates can be much higher than when using conventional furnaces. However, MEMS holders suffer from limited fields of view and restrictions on specimen geometry.[19,20]

On the Titan ETEM at DTU Cen, stable flow of each gas component is ensured using digital mass flow controllers on each gas line leading into a manifold system. Gas–gas reactions in the inlet system are assumed to be negligible. The high degree of stability provided by accurate control of gas injection into the sample region allows specific specimen areas to be followed over extended periods of time, providing a better timeline of data from individual sample regions, such as metal particles. Furthermore, high resolution images can then be acquired at elevated temperature without the compromise of short acquisition times.

Experimental considerations

Before starting an *in situ* experiment using an ETEM, several experimental issues have to be considered and addressed. In an ETEM, the parameter space is much larger than that in a conventional TEM. In addition to the usual microscope parameters, total gas pressure, gas composition and specimen temperature have to be optimised for the gas–solid interaction of interest. Furthermore, the temporal aspect of dynamic studies has to be accounted for. In order to increase the chance of success of an *in situ* experiment, it should first be carried out *ex situ* to assess whether the desired reaction can be achieved in the ETEM. In addition, gas–solid interactions that are carried out in an ETEM are invariably influenced by the electron beam. Interactions with the gas of both the incident high energy electrons and low energy secondary electrons emitted from the specimen can cause ionisation of the gas molecules, thereby changing their reactivity. All *in situ* TEM experiments should therefore be verified by performing parallel experiments in the absence of the electron beam, either in the TEM or in a reactor outside the microscope.

The sample region in the microscope column can be considered as a gas reactor, in which the gases that are used in the experiment should be of high purity and the vacuum level should be assessed to limit possible contaminants. It is good practice to separate oxidising and reducing experiments, for example by using extended cleaning and pumping periods, including baking and plasma cleaning of the sample region and

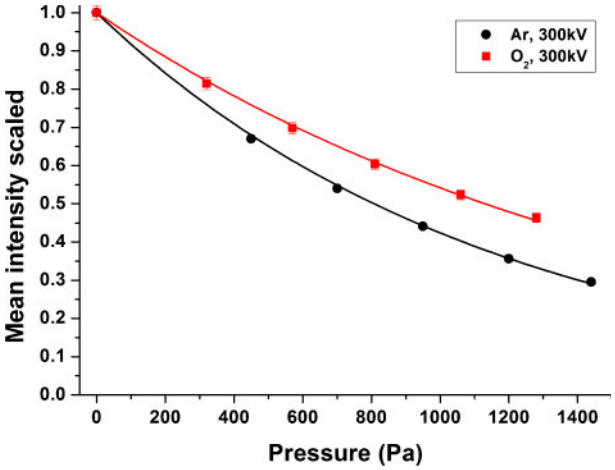

2 Normalised image intensity (without specimen present) measured on pre-GIF UltraScan CCD camera, plotted as function of gas pressure for Ar and O_2. Primary electron energy is 300 keV. Data points have been fitted to exponential functions

the gas inlet system. Continuous monitoring of the gas composition can aid in tracking and explaining artefacts observed during *in situ* experiments.

As illustrated in Fig. 2, the intensities in recorded images decrease with increasing gas pressure, the more so for heavier gas molecules. At a gas pressure of 1400 Pa of Ar, the image intensity is more than 70% lower than that in high vacuum ($<10^{-5}$ Pa). Scattering of primary electrons by gas molecules also results in a loss of coherence and thereby a loss of image resolution. Whereas these effects are not as pronounced for lighter gases such as oxygen and hydrogen, they must still be considered when designing experiments and when analysing contrast in high resolution TEM and scanning TEM images quantitatively. Similarly, energy losses resulting from interactions between primary electrons and gas molecules can introduce many features into EELS spectra in the region up to ~25 eV (see section on '*In situ* monochromated EELS' and Fig. 6). *In situ* experiments that involve the use of a gaseous environment and an elevated specimen temperature also require a careful choice of holders and grids to ensure stability in the presence of gas flow, as outlined above.

In order to monitor the gases to which the sample is exposed, the microscope contains a capillary, whose opening is in the immediate vicinity of the sample inside the objective lens. This capillary is heated and pumped separately using a turbomolecular pump. Owing to the large pressure drop (~6 orders of magnitude) along the 1·6 mm capillary, it is possible to measure the gas composition directly using a quadrupole mass spectrometer (residual gas analyser: RGA). The response time from changing the gas flow or composition using the mass flow controllers until it is measured using the RGA is on the order of seconds. The RGA is used primarily to monitor the cleanliness of the gas introduced into the microscope.

During bake-out of the system, the interior of the microscope is exposed to gases desorbing from the inlet system. The Titan ETEM is equipped with an internal plasma cleaner (Evactron 45 decontaminator). The removal of carbon contamination by plasma cleaning

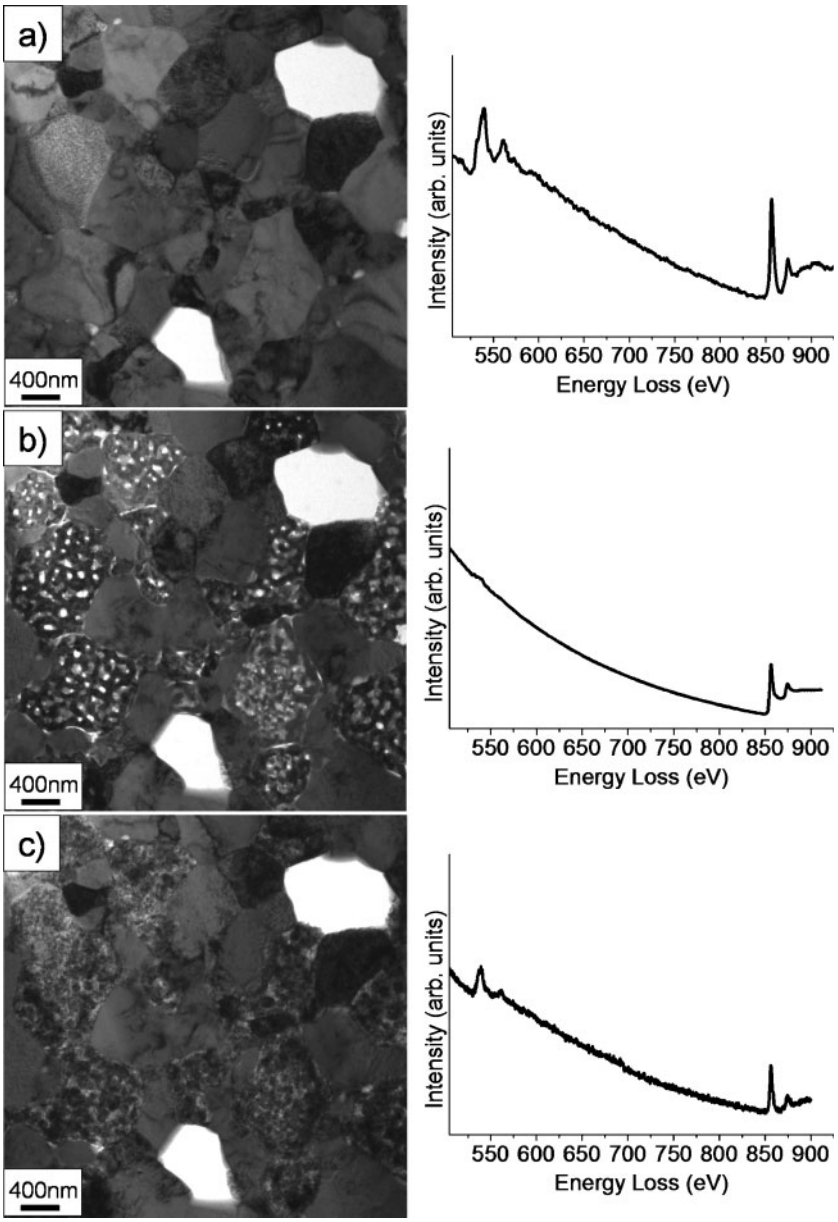

a before reduction at room temperature in normal TEM mode; *b* after *in situ* reduction in 130 Pa H_2 at 500°C for 2 h; *c* after *in situ* reoxidation in 320 Pa O_2 at 500°C for 2 h

3 Bright field images acquired during *in situ* reduction and reoxidation of Ni-YSZ SOFC anode: corresponding EELS spectra are shown next to each image

should be considered a standard procedure before each session of *in situ* environmental electron microscopy.

Selected applications

The considerations outlined above should be taken into account when applying environmental transmission microscopy as a technique for material research. A selection of representative applications, in which the above considerations are a natural part of the experimental procedure, is now presented. The results illustrate the performance of the Titan ETEM for different applications. More detailed accounts are presented elsewhere.

In situ reduction of metal oxides

Solid oxide fuel cell (SOFC) technology is often based on the use of anodes that are made from nickel–yttria stabilised zirconia (Ni-YSZ) cermets. The Ni is initially in its oxidic state (NiO) during SOFC production and is reduced to metallic Ni during the first cycle of operation. As the microstructure of the anode influences the electrochemical performance of the cell,[21] as well as its stability for long term use,[22] the nature of the microstructural changes that occur during this phase change is of interest. Furthermore, reoxidation of the Ni can occur as a result of high fuel consumption, air leakage or uncontrolled shutdowns. The resulting volume change from Ni to NiO can be detrimental to the microstructure of the thin supported electrolyte[23] and can lead to failure of the entire device.

In order to gain insight into the reduction and reoxidation process, a thin TEM lamella was prepared using a standard focused ion beam procedure and examined *in situ* in the ETEM.[24] Figure 3 shows bright field TEM images of an area consisting of NiO and YSZ grains. *In situ* treatment of the sample in 130 Pa of H_2 at

temperatures of up to 500°C was used to follow the reduction of the NiO grains and the resulting formation of porosity. Diffraction patterns showed an epitaxial relationship between the NiO grains and the growing metallic Ni (shown elsewhere[24]). Electron energy-loss spectroscopy was used to monitor the decrease in the oxygen *K*-ionisation edge and to show that the Ni L_3/L_2 ratio also decreased.[25] The sample was then treated *in situ* in 320 Pa of O_2 at temperatures of up to 500°C in order to reoxidise the metallic Ni grains, as shown in Fig. 3. During the reoxidation process, the pores that had been created in the grains were refilled. The growing NiO was polycrystalline, and the oxygen *K*-ionisation edge was observed to increase. Although the YSZ grains did not appear to change chemically, stress from the volume change in the Ni containing grains was observed in the form of diffraction contrast variations in the YSZ grains. The volume decrease resulting from the reduction of NiO to metallic Ni was compensated by the formation of pores. Reoxidation of metallic Ni to polycrystalline NiO grains induced stress in the matrix, cracking of the structure and ultimately device failure.

Particle formation and migration

Many industrial catalysts are prepared using wet chemical processes, with metals added in solution followed by calcination and reduction to form the active material. A high degree of control in each of these steps is crucial.

An important deactivation mechanism in supported metal catalysts is sintering, in which the average particle size increases, leading to a decrease in active surface area.[26] Several mechanisms have been suggested, but the difficulty of local high spatial resolution characterisation has hampered experimental verification. Recently, it has become possible to expose metal particles on a substrate at elevated temperatures to a gaseous environment in the TEM to follow growth processes in real time at high resolution.

Two possible schemes for sintering are generally considered:

(i) in Ostwald ripening, the particles are immobile, and net mass transport from smaller to larger particles occurs by the diffusion of single atoms or molecular species

(ii) in particle migration and coalescence, entire particles migrate over the surface of the support and coalesce when they are in close proximity.

In order to distinguish between these possible mechanisms, a model catalyst was made by sputter coating gold onto electron transparent flakes of boron nitride and exposed to 130 Pa of H_2 at 400°C in the ETEM. Such a system mimics the more complicated structures found in industrial catalyst systems.

Figure 4 shows six frames taken from a movie recorded under these conditions. From Fig. 4*a* to *b*, particles 1 and 2 are observed to coalesce. In Fig. 4*b* and *c*, the same phenomenon is observed for particle 3. From Fig. 4*c* to *f*, particle 4 gradually becomes smaller, indicating that Ostwald ripening is taking place. The temporal resolution in these images does not allow intermediate states of coalescence, which take place over timescales that are much shorter than those involved in particle migration, to be observed. However, this study highlights the fact that both sintering mechanisms can take place under the same conditions. Based on such investigations, activation energies can be measured by relating the observed dynamics to the local specimen temperature.

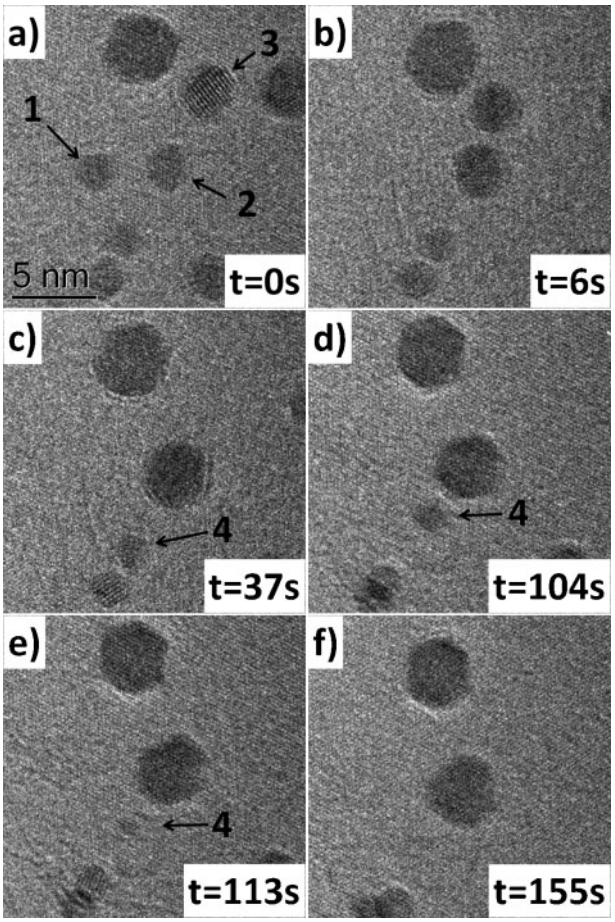

4 Frames taken from sequence of bright field images of gold particles on boron nitride support imaged in 130 Pa of H_2 at 410°C: images were recorded using 300 kV primary electron beam with C_S set to below 5 μm (see text for more details)

C_S correction for improved image interpretability

The ETEM at DTU Cen is equipped with an image C_S corrector that allows a choice of spherical aberration coefficient of the objective lens system. In principle, for a fully aligned corrector system, a point to point resolution of better than 0·1 nm is achievable. However, when examining specimens at elevated temperature in the presence of gas, the resolution and information limit are affected by the stability of the combined system, which includes the microscope, the holder and the sample itself. In addition, elastic and inelastic scattering of the electron beam by gas molecules degrades image resolution. Fourier transforms of lattice fringe images can be used as a measure of the stability of the system.

Figure 5 shows a representative lattice fringe image acquired in ETEM mode with its corresponding Fourier transform, which indicates that the recorded image contains lattice fringes with spacings below 0·14 nm. Correction of the spherical aberration of the objective lens system has the additional advantage of minimising image delocalisation, especially near the edges of

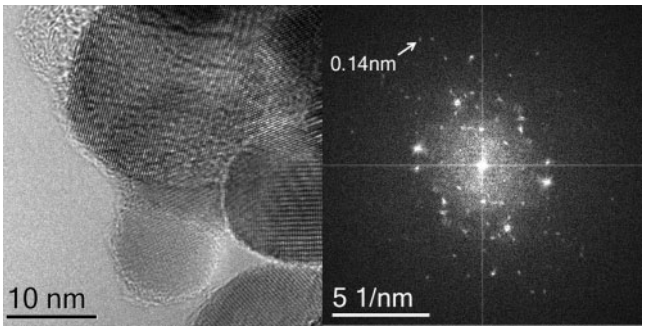

5 High resolution lattice image of ZrO_2 particles in 1 : 1 mixture of H_2 and N_2 recorded at total gas pressure of 310 Pa and at specimen temperature of 177°C: Fourier transform provides indication of stability of microscope and specimen under these conditions

crystals, making surface and facet structures more directly interpretable.[27] However, the full quantitative analysis of such images requires a detailed knowledge of the path of the electron along the microscope column in the presence of gas in the objective lens both above and below the sample.[28] The factors that affect this path and its effect on image contrast will be explored in more detail in future studies.

In situ monochromated EELS

The combination of *in situ* capabilities and a monochromated electron source allows for the acquisition of EELS data with improved energy resolution, as well as providing an opportunity to follow gas–solid interactions spectroscopically and spatially. Whereas the decreased beam intensity poses a challenge for monochromated EELS studies of core losses, it is less of an issue in the low loss region. For example, the low loss EELS region of an NiZn sample used for the selective hydrogenation of acetylene[29] reveals different features when studying the as prepared sample and the *in situ* reduced sample, as shown in Fig. 6*a* before and after reduction of the oxide. The corresponding TEM images are shown in Fig. 6*b*. The fresh sample consists of a mixture of Ni and Zn oxides. After reduction, metallic NiZn particles are formed, changing the coordination of the Ni and Zn atoms and thereby altering the electronic state of the sample and leading to changes in the energy-loss spectrum. The spectrum of the as prepared sample shows features at 3·6–5·0 eV that are difficult to resolve without the use of the monochromator due to the broad tail of the zero loss peak. These features are not present in the spectrum of the reduced sample. The peak observed at 12 eV in the spectrum of the reduced sample is the H *K*-ionisation edge described by the Lyman series[30] convolved with instrument broadening. By studying low loss EELS features in combination with high resolution TEM images acquired in the presence of a gas, information about changes in the valence state of the solid material can be obtained. When combined with theoretical models, a more complete picture can be presented.

Besides using EELS to measure variations in composition and valence state, spectra can also be used to measure gas pressure, and interesting additional features are revealed in spectra acquired from gases when using the monochromator, as shown in Fig. 7 for molecular nitrogen. Although the energy resolution is not as high as that achieved in the extensive dedicated EELS work of Hitchcock and co-workers (e.g. Ref. 31) spectra can be acquired in the ETEM at the same time as acquiring aberration corrected lattice images.

Summary

In situ ETEM has come a long way since the pioneering work of Baker and Harris.[1] Developments in instrumentation now allow atomic resolution images to be acquired digitally at high frame rates in combination with high energy resolution spectroscopy and techniques such as annular dark field imaging and electron tomography. These new capabilities must, however, be applied with considerable care. It is especially important to understand differences between chemical reactions performed *ex situ* and those performed in the electron

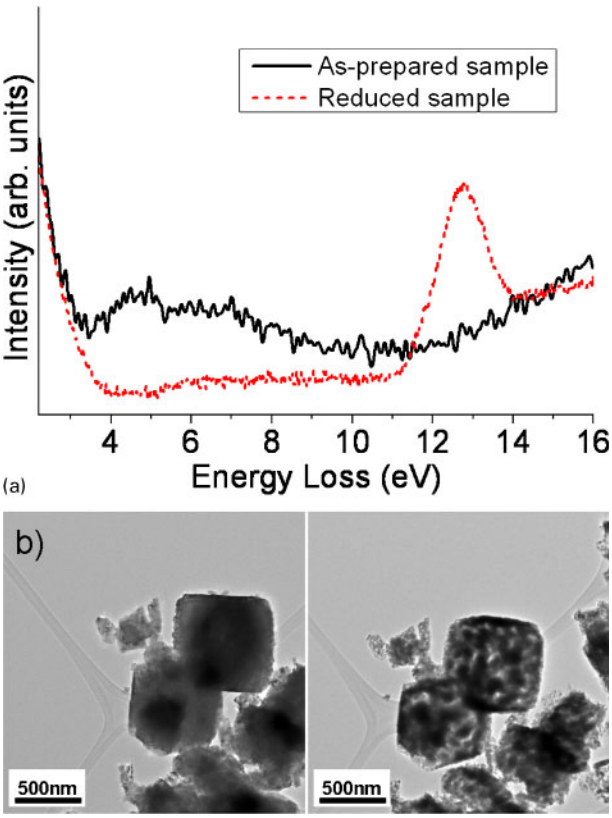

a low loss EELS of NiZn sample before (in high vacuum) and after (120 Pa H_2, T=450°C) *in situ* reduction; *b* TEM images of corresponding as prepared (left) and reduced (right) samples

6 Monochromated electron energy-loss spectra and corresponding images acquired in environmental TEM

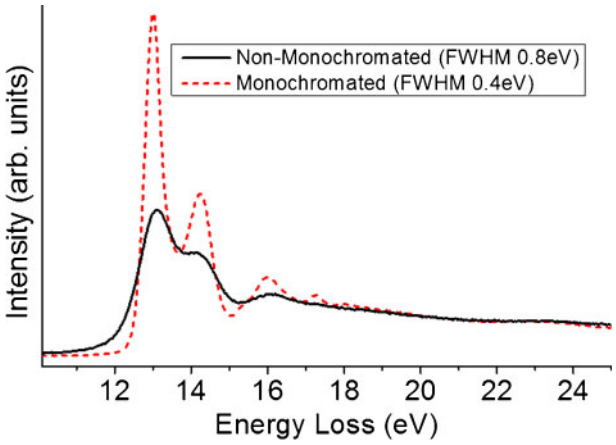

7 Non-monochromated and monochromated EELS of N_2 gas acquired *in situ* at 500 Pa at room temperature

microscope in the presence of the high energy electron beam.

Acknowledgements

The A. P. Møller and Chastine Mc-Kinney Møller Foundation is gratefully acknowledged for its contribution towards the establishment of the Center for Electron Nanoscopy in the Technical University of Denmark. Quentin Jeangros, Aïcha Hessler-Wyser, Antonin Faes, Jan Van herle and Jan-Dierk Grunwaldt are gratefully acknowledged for providing samples and for ongoing collaborations. Jörg Jinschek, Stephan Kujawa and Mathijs de Moor are gratefully acknowledged for assistance, fruitful discussions and comments.

References

1. R. T. K. Baker and P. S. Harris: 'Controlled atmosphere electron-microscopy', *J. Phys. E, Sci. Instrum.*, 1972, **5**, (8), 793.
2. E. D. Boyes and P. L. Gai: 'Environmental high resolution electron microscopy and applications to chemical science', *Ultramicroscopy*, 1997, **67**, (1–4), 219.
3. A. K. Datye: 'Electron microscopy of catalysts: recent achievements and future prospects', *J. Catal.*, 2003, **216**, (1–2), 144.
4. S. Kodambaka, J. Tersoff, M. C. Reuter and F. M. Ross: 'Germanium nanowire growth below the eutectic temperature', *Science*, 2007, **316**, 729.
5. H. Hashimoto and T. Naiki: 'High temperature gas reaction specimen chamber for an electron microscope', *Jpn J. Appl. Phys.*, 1968, **7**, (8), 946.
6. R. T. K. Baker, F. S. Feates and P. S. Harris: 'Continuous electron-microscopic observation of carbonaceous deposits formed on graphite and silica surfaces', *Carbon*, 1972, **10**, (1), 93.
7. R. T. K. Baker: '*In situ* electron-microscopy studies of catalyst particle behavior', *Catal. Rev.–Sci. Eng.*, 1979, **19**, (2), 161.
8. R. Sharma: 'An environmental transmission electron microscope for in situ synthesis and characterization of nanomaterials', *J. Mater. Res.*, 2005, **20**, (7), 1695.
9. C. Kisielowski, E. Principe, B. Freitag and D. Hubert: 'Benefits of microscopy with super resolution', *Physica B, Condens. Mater.*, 2001, **308–310**, 1090.
10. D. S. Su, T. Jacob, T. W. Hansen, D. Wang, R. Schlogl, B. Freitag and S. Kujawa: 'Surface chemistry of Ag particles: Identification of oxide species by aberration-corrected TEM and by DFT calculations', *Angew. Chem. Int. Ed.*, 2008, **47**, (27), 5005.
11. H. Boersch, J. Geiger and H. Hellwig: 'Steigerung Der Auflösung Bei Der Elektronen-Energieanalyse', *Phys. Lett.*, 1962, **3**, (2), 64.
12. C. Mitterbauer, G. Kothleitner, W. Grogger, H. Zandbergen, B. Freitag, P. Tiemeijer and F. Hofer: 'Electron energy-loss near-edge structures of 3d transition metal oxides recorded at high-energy resolution', *Ultramicroscopy*, 2003, **96**, (3–4), 469.
13. W. Grogger, F. Hofer, G. Kothleitner and B. Schaffer: 'An introduction to high-resolution EELS in transmission electron microscopy', *Topics Catal.*, 2008, **50**, (1–4), 200.
14. http://www.fei.com
15. M. Hammar, F. K. LeGoues, J. Tersoff, M. C. Reuter and R. M. Tromp: '*In situ* ultrahigh vacuum transmission electron microscopy studies of hetero-epitaxial growth. Part 1: Si(001)/Ge', *Surf. Sci.*, 1996, **349**, (2), 129.
16. B. J. Kim, J. Tersoff, S. Kodambaka, M. C. Reuter, E. A. Stach and F. M. Ross: 'Kinetics of individual nucleation events observed in nanoscale vapor–liquid–solid growth', *Science*, 2008, **322**, (5904), 1070.
17. M. Lin, J. P. Y. Tan, C. Boothroyd, K. P. Loh, E. S. Tok and Y. L. Foo: 'Direct observation of single-walled carbon nanotube growth at the atomistic scale', *Nano Lett.*, 2006, **6**, (3), 449.
18. M. Lin, J. P. Y. Tan, C. Boothroyd, K. P. Loh, E. S. Tok and Y. L. Foo: 'Dynamical observation of bamboo-like carbon nanotube growth', *Nano Lett.*, 2007, **7**, (8), 2234.
19. L. F. Allard, K. L. More and J. Liu: 'Applications of high-resolution aberration-corrected STEM imaging to studies of the behavior of nanophase materials at elevated temperatures', *Microsc. Microanal.*, 2009, **15**, (Suppl 2), 130.
20. J. Liu, J. Braddock-Wilking and L. F. Allard: 'In-situ synthesis of PtSn/C fuel cell nanocatalysts in an aberration-corrected STEM/TEM', *Microsc. Microanal.*, 2009, **15**, (Suppl 2), 688.
21. S. C. Singhal and K. Kendall(eds.): 'High temperature solid oxide fuel cells – fundamentals, design and applications'; 2003, Amsterdam, Elsevier.
22. D. Simwonis, F. Tietz and D. Stover: 'Nickel coarsening in annealed Ni/8YSZ anode substrates for solid oxide fuel cell', *Solid State Ionics*, 2000, **132**, (3–4), 241.
23. A. Faes, A. Nakajo, A. Hessler-Wyser, D. Dubois, A. Brisse, S. Modena and J. van Herle: 'Redox study of anode-supported solid oxide fuel cell', *J. Power Sources*, 2009, **193**, (1), 55.
24. Q. Jeangros, A. Faes, J. B. Wagner, T. W. Hansen, U. Aschauer, J. van Herle, A. Hessler-Wyser and R. E. Dunin-Borkowski: '*In situ* redox cycle of a nickel-YSZ fuel cell anode in an environmental TEM', *Acta Mater.*, 2010, **58**, 4578–4589.
25. T. W. Hansen: 'Sintering and particle dynamics in supported metal catalysts', PhD thesis, Technical University of Denmark, Lyngby, Denmark, 2002.
26. P. Wynblatt and N. A. Gjostein: 'Supported metal crystallites', *Prog. Solid State Chem.*, 1975, **9**, 21.
27. B. Freitag, S. Kujawa, P. M. Mul, J. Ringnalda and P. C. Tiemeijer: 'Breaking the spherical and chromatic aberration barrier in transmission electron microscopy', *Ultramicroscopy*, 2005, **102**, (3), 209.
28. H. Yoshida and S. Takeda: 'Image formation in a transmission electron microscope equipped with an environmental cell: single-walled carbon nanotubes in source gases', *Phys. Rev. B*, 2005, **72B**, (19), 195428.
29. F. Studt, F. Abild-Pedersen, T. Bligaard, R. Z. Sørensen, C. H. Christensen and J. K. Nørskov: 'Identification of non-precious metal alloy catalysts for selective hydrogenation of acetylene', *Science*, 2008, **320**, (5881), 1320.
30. R. F. Egerton: 'Electron energy-loss spectroscopy in the electron microscope'; 1996, Berlin, Springer.
31. A. P. Hitchcock and D. C. Mancini: 'Bibliography and database of inner shell excitation spectra of gas phase atoms and molecules', *J. Electron Spectrosc. Relat. Phenom.*, 1994, **67**, (1), 1.